

*Please share your stories about how Open Access to this article benefits you.*

# In vivo photoacoustic imaging of chemotherapy-induced apoptosis in squamous cell carcinoma using a near-infrared caspase-9 probe

by Quihong Yang et al.

2011

This is the published version of the article, made available with the permission of the publisher. The original published version can be found at the link below.

Quihong Yang et al. (2008). In vivo photoacoustic imaging of chemotherapy-induced apoptosis in squamous cell carcinoma using a near-infrared caspase-9 probe. *Journal of Biomedical Optics* (16)11:116026.

Published version: <http://www.dx.doi.org/10.1117/1.3650240>

Terms of Use: <http://www2.ku.edu/~scholar/docs/license.shtml>

# *In vivo* photoacoustic imaging of chemotherapy-induced apoptosis in squamous cell carcinoma using a near-infrared caspase-9 probe

QiuHong Yang,<sup>a</sup> Huizhong Cui,<sup>b</sup> Shuang Cai,<sup>a</sup> Xinmai Yang,<sup>b</sup> and M. Laird Forrest<sup>a</sup>

<sup>a</sup>University of Kansas, Department of Pharmaceutical Chemistry, 2095 Constant Avenue, Lawrence, Kansas 66047

<sup>b</sup>University of Kansas, KU Bioengineering Research Center and Department of Mechanical Engineering, 1530 West 15th Street, Lawrence, Kansas 66045

**Abstract.** Anti-cancer drugs typically exert their pharmacological effect on tumors by inducing apoptosis, or programmed cell death, within the cancer cells. However, no tools exist in the clinic for detecting apoptosis in real time. Microscopic examination of surgical biopsies and secondary responses, such as morphological changes, are used to verify efficacy of a treatment. Here, we developed a novel near-infrared dye-based imaging probe to directly detect apoptosis with high specificity in cancer cells by utilizing a noninvasive photoacoustic imaging (PAI) technique. Nude mice bearing head and neck tumors received cisplatin chemotherapy (10 mg/kg) and were imaged by PAI after tail vein injection of the contrast agent. *In vivo* PAI indicated a strong apoptotic response to chemotherapy on the peripheral margins of tumors, whereas untreated controls showed no contrast enhancement by PAI. The apoptotic status of the mouse tumor tissue was verified by immunohistochemical techniques staining for cleaved caspase-3 p11 subunit. The results demonstrated the potential of this imaging probe to guide the evaluation of chemotherapy treatment. © 2011 Society of Photo-Optical Instrumentation Engineers (SPIE). [DOI: 10.1117/1.3650240]

Keywords: photoacoustic imaging; apoptosis; caspase; *in vivo*; cancer imaging.

Paper 11195LRR received Apr. 15, 2011; revised manuscript received Sep. 19, 2011; accepted for publication Sep. 20, 2011; published online Oct. 27, 2011.

## 1 Introduction

Noninvasive imaging techniques are necessary for early cancer detection and evaluation of the chemotherapeutic effect on tumors. Current diagnostic imaging techniques generally include  $\gamma$ -scintigraphy, magnetic resonance imaging, computed tomography, and ultrasonography; however, these techniques only give morphological information on the tumor. These techniques do not report the biochemical response of the tumor to treatment and physical changes in the tumor in response to treatment may take days to weeks to fully manifest. Positron emission topography and SPECT can indirectly detect tumor response to treatment due to changes in metabolic activity and blood perfusion, respectively. However, no clinical imaging technique can directly detect the biochemical response, e.g., apoptosis, of tumors to treatment. Since apoptosis often occurs within the first 18 to 36 h after treatment, direct imaging of apoptosis would rapidly indicate if there is a response in the tumor to chemotherapy.

Photoacoustic imaging (PAI) overcomes the spatial and resolution limitations of conventional imaging techniques at a relatively low cost,<sup>1,2</sup> and it has shown its potential to monitor the growth of melanoma brain tumors<sup>3</sup> and melanoma metastasis in sentinel lymph nodes.<sup>4</sup> However, ascribed to the fact that PAI utilizes the optical absorption of tissues for contrast, it cannot differentiate normal from cancerous cells unless the cells are overexpressing chromomeric marker (e.g., melanomas) or labeled by reporter moieties as contrast agent to enhance the contrast between normal and pathological tissues. In this case,

application of a contrast agent such as fluorochromes is expected to facilitate both the visualization of head and neck squamous cell carcinoma (HNSCC) cancer cells and their response to treatment *in vivo* by PAI.

We have synthesized a near-infrared fluorescent imaging probe – IR780-linker-Val-Ala-Glu(OMe)-FMK by conjugating a fluorochrome (IR780) to Z-Val-Ala-Glu (OMe), a cell permeable caspase inhibitor. The activation of caspase family of cysteine proteases has been recognized as a critical event of apoptosis, which is a physiological process of type I programmed cell death. Typically anti-cancer agents act on cancer cells to induce apoptosis, so apoptosis is a rapid and definite indicator of tumor response. For this reason, apoptosis is used in screening drug candidates in cell culture. The fluoromethyl ketone of the tripeptides valine, alanine, and O-methylglutamic acid [Val-Ala-Glu(OMe)-FMK] can specifically and irreversibly bind to the cysteine residue at the active site of caspase-9.<sup>5</sup> Our preliminary *in vitro* cell-imaging test with prostate cancer DU 145 cells demonstrated the sensitivity of this imaging probe for cell apoptosis.<sup>6</sup> In this study, we evaluated the application of IR780-linker-Val-Ala-Glu(OMe)-FMK for PAI to detect procaspase-9 activation caused by anticancer drug treatment in living nude mice bearing HNSCC tumors.

## 2 Materials and Methods

### 2.1 Photoacoustic Imaging System

The mechanism of the PAI system was previously described<sup>2,3</sup> and is identical to the system presented by Song et al.<sup>1</sup> A

Address all correspondence to: M. Laird Forrest, University of Kansas, Department of Pharmaceutical Chemistry, 2095 Constant Avenue, Lawrence, Kansas 66047. Tel: +1 (785) 864-4388; Fax: +1 (785) 864-5736; E-mail: mforrest@ku.edu.

tunable OPO laser (Surelite OPO PLUS; Continuum, Santa Clara, California) pumped by a Q-switched Nd:YAG laser (Surelite; Continuum, Santa Clara, California) is used to generate the laser pulse with a repetition rate of 10 Hz and a laser wavelength of 680 nm. The laser light, directed by a prism group, forms a ring-shaped illumination on an optical condenser and is then refocused by a conical lens on the targeted area. The produced photoacoustic signals are collected by a 5-MHz single-element focused ultrasonic transducer (SU-108-013, Sonic Concepts, Bothell, Washington), amplified by a pre-amplifier (5072PR, Olympus-NDT, Waltham, Massachusetts), and finally collected by a personal computer through an A/D Scope Card (CS21G8-256MS, Gage, Lockport, Illinois) with a 125-MHz sampling rate to reconstruct 2-D images. The 5-MHz ultrasonic transducer (fractional bandwidth of 60%, 35-mm focal length, and 33-mm aperture size) is mounted in the center of the condenser and driven by a step motor to scan over the targeted region. It takes ca. 20 min to scan a 20 mm × 20 mm area. Previous work<sup>2,3</sup> on this system has shown that it has a lateral resolution of 270  $\mu\text{m}$  and an axial resolution of 220  $\mu\text{m}$ .

## 2.2 Imaging Agent

The near-infrared fluorescent imaging agent – IR780-linker-Val-Ala-Glu(OMe)-FMK (NIR-FMK) was synthesized in our laboratory.<sup>6</sup> The imaging agent had a maximum absorption wavelength at 640 nm and emission wavelength at 729 nm with a quantum yield of 0.75. Sensitivity of this imaging agent for cell apoptosis imaging was tested by *in vitro* cell imaging. Cellular uptake of NIR-FMK was compared between normal prostate cancer DU-145 cells and anticancer treated DU-145 cells. The results demonstrated that cancer cells undergoing apoptosis presented a significant signal when they were fluorescently imaged, resulting from uptake of the imaging agent; while normal cancer cells showed the concentration dependent uptake of it. (Qualification of this dye for fluorescent imaging is described elsewhere.<sup>6</sup>)

## 2.3 Tumor Model

Female Nu/Nu mice used in the experiments were maintained under the supervision and guidelines of the University of Kansas Institutional Animal Care and Use Committee. Animals were fed on a diet of low chlorophyll feed for at least two weeks before imaging. Human HNSCC cells, MDA-1986, were prepared in 1×PBS solution at a cell concentration of  $2 \times 10^7$  cells/mL. Nude mice were anesthetized with 1.5% isoflurane in oxygen-air mixture (50:50). Fifty microliters of cell suspension was injected into the sub-mucosa of a mouse using a 30-ga needle. Primary HNSCC tumors were observed on the cheek of the animals two weeks after implantation with a size range of 5 to 150 mm<sup>3</sup> [tumor volume =  $0.52 \times (\text{width})^2 \times (\text{length})$ ]. Animals were euthanized at the completion of the study.

## 2.4 Treatment and Fluorescent Imaging

Female nude mice bearing head and neck tumors were randomly divided into two groups, including cisplatin treatment and control groups. One dose of 10.0-mg/kg cisplatin (LC Laboratories) was intravenously administered via the tail vein to the animals in the treatment group once the tumor size was between 40 to

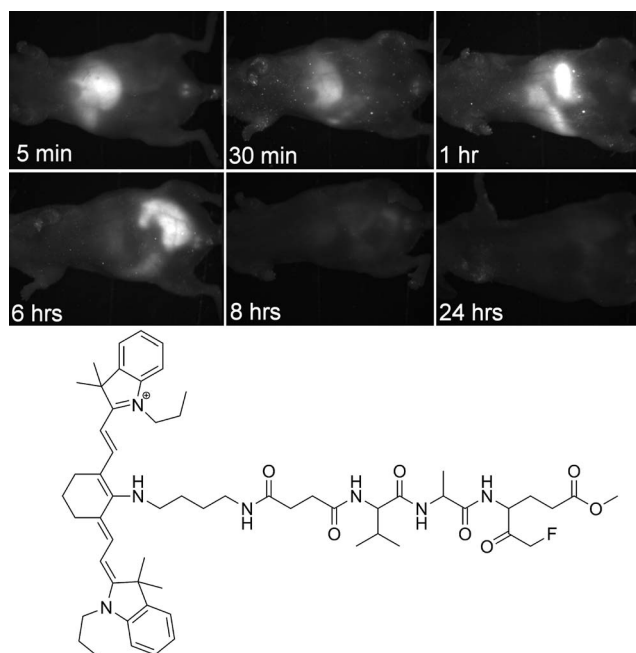


**Fig. 1** Fluorescent images of systemic clearance of NIR-FMK contrast agent. Animal was fluorescently imaged after tail vein injection of 25 nmol of NIR-FMK. Agent rapidly cleared from the systemic circulation and was concentrated in the liver from 5 to 30 min and in the intestines from 1 to 6 h. The structure of NIR-FMK is shown in the bottom panel.

50 mm<sup>3</sup>. The control group received no treatment. NIR-FMK (25 nmol in 100- $\mu\text{L}$  of saline) was intravenously injected via the tail vein into a tumor-negative mouse, and systemic clearance of the dye was evaluated by fluorescent imaging (CRI Maestro Flex, CRI Inc., Woburn, Massachusetts) throughout 5 min to 24 h. A 575 to 605-nm filtered halogen excitation light and a 645-nm long pass emission filter were applied. Fluorescence intensity in the abdominal area was measured using a cooled charge-coupled-device (CCD) camera with auto exposure (Fig. 1). The unscaled images were normalized to the same exposure and the brightness and contrast were adjusted for print.

## 2.5 In Vivo Photoacoustic Imaging

Twenty-four hours post-treatment with cisplatin, mice were positioned as shown in Fig. 2 (top) and anesthetized by inhalation of a mixture of 1% isoflurane and pure oxygen at 1-L/min flow rate. The initial background photoacoustic (PA) images were obtained around the tumor region on the cheek of the mouse and then NIR-FMK (25 nmol in 100  $\mu\text{L}$  of saline) was intravenously injected via the tail vein. PA images were acquired at 2, 4, 6, and 8 h. A laser wavelength of 680 nm was used during the imaging, and the imaging depth was 2 to 3 mm. Signal intensity was analyzed using Fiji/ImageJA software (ver. 20110307, <http://pacific.mpi-cbg.de/wiki/index.php/Fiji>).

## 2.6 Immunostaining for Apoptosis

The HNSCC tumor was excised within several hours after PAI. Subsequently, it was embedded into tissue freezing medium (Triangle Biomedical Sciences, Durham, North Carolina) and sectioned using a cryostat (Thermo Shandon Limited,

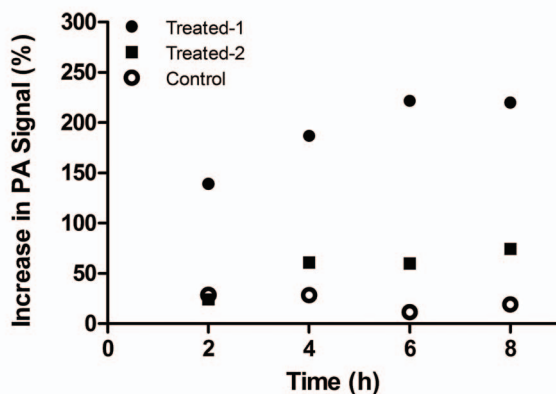


**Fig. 2** Increase in PA amplitude within the HNSCC tumor after intravenous injection of imaging agent via the tail vein. The treated animals ( $n = 2$ ) were intravenously given 10 mg/kg of cisplatin 24 h prior to administration of the imaging agent. PAI images were centered on the tumor (circle, bottom). Images of the control animal ( $n = 1$ ) at the optimal imaging depth were chosen for data analysis.

Kalamazoo, Michigan). Fourteen micron (thickness) sections of the tumor tissue were stained with a goat primary polyclonal antibody for cleaved caspase-3 p11 subunit (Asp-175-Ser-176) and a donkey anti-goat secondary antibody with a fluorescein isothiocyanate (FITC) fluorophore (Santa Cruz Biotechnology Inc., Santa Cruz, California). Cell nuclei were stained with 4',6-diamidino-2-phenylindole (DAPI).

### 3 Results and Discussion

Systemic clearance of the imaging agent from a tumor-free mouse was evaluated by injecting animals with 25 nmol of NIR-FMK via their tail vein and fluorescently imaging animals from 5 min to 24 h. Fluorescence signals in the abdominal area shown in Fig. 1 indicated that NIR-FMK was retained by the liver within the first 5 min after injection, with later distribution to the small intestines and spleen. Organ fluorescence decreased to background or autofluorescence levels after eight hours, indicating that the agent had been completely cleared from the body. The kinetics of clearance of NIR-FMK served to assist with determining the time course of PA imaging on tumor-positive mice. Within the first hour, the liver had cleared the imaging agent from the systemic circulation, offering a favorable time frame for PA imaging to differentiate the imaging agents bound to the tumor tissue from the free agent distributed in the tissue space. In addition, considering the imaging resolution and patients' comfort in future clinical applications, we performed the PA imaging at 2, 4, 6, and 8 h after intravenous injection.

Maximum amplitude projection images obtained from the PAI of the HNSCC tumor region shown in Fig. 2 were converted to grayscale images. The grayscale images at various time points were linearly aligned using the scale-invariant feature transform function of Fiji/ImageJA software (ver. 20110307, <http://pacific.mpi-cbg.de/wiki/index.php/Fiji>) (Fig. 3). Quantification of PA signal intensity within the tumor region was performed in triplet for each image by measuring the mean gray value (units: gray/pixel) of the circled tumor region. The extent of signal enhancement was calculated by normalizing the tumor signal against a background reading taken immediately before injection of the imaging agent (Fig. 2), and the process can be indicated with the following equation:

$$\text{Increase in PA signal} = \frac{[(\text{intensity of each time point} - \text{intensity of background image}) / \text{intensity of background imaging}] \times 100\%.$$

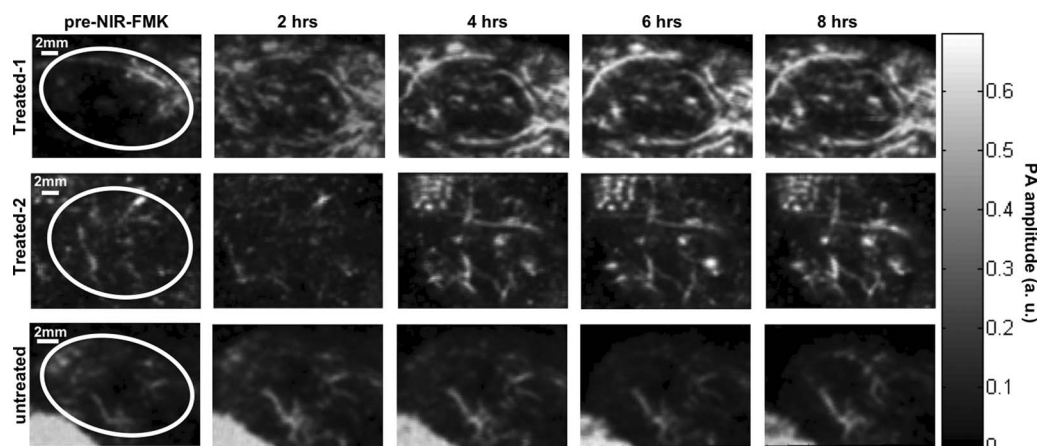


**Fig. 3** PA images of HNSCC tumor apoptosis after contrast treatment. Animals were administered 25 nmol of NIR-FMK via the tail vein. Intravenous cisplatin (10 mg/kg) was administered 24 h prior to imaging in the treatment group.



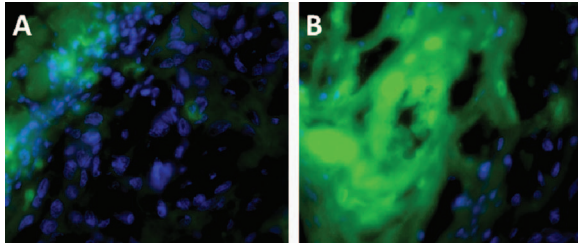


**Fig. 4** Immunostaining for apoptosis in tumor. (a) Representative control section stained with secondary antibody alone and (b) tissue section of the HNSCC tumor stained for caspase-3 p11 subunit after cisplatin treatment. Green FITC fluorescence indicates the presence of apoptotic cells and blue DAPI indicates the cell nuclei.

The signal intensity within the tumor region of each frame (denoted by a white circle in Fig. 3) was compared with other frames in the same time series between the treated and control groups. The same scaling was used for all images within the series. The triangle-shaped white region in the lower left corner of the control group images in Fig. 3 is noise from a piece of paper used to cover the right eye, which is outside of the HNSCC tumor region.

The signal of the mouse in the control group reached the maximum intensity at 2 h and after that it began to drop. This indicated that the imaging probe was nonspecifically distributed to the tumor tissues after injection, and the agent then cleared with the systemic circulation as observed in the fluorescence studies (Fig. 1). By comparison, PA images of the treatment group demonstrated enhanced signal intensity during the same time course. The significant difference between control and cisplatin treatment groups could be explained by the specific and irreversible binding between NIR-FMK and caspase 9 in the tumor tissue. In cisplatin treated mice, apoptosis of HNSCC cancer cells resulted in the activation of caspase 9 around the tumor, serving as binding sites for the imaging probe and allowing the probe to accumulate.<sup>7</sup> Since the control group did not receive the chemotherapy treatment, caspase 9 was not activated due to the lack of the cell apoptosis process and the imaging probe was rapidly cleared from the tumor. Diffuse contrast on the peripheral of the tumor region in the treated group is likely due to apoptosis of metastatic cells on the margins of the solid primary tumor mass.

Apoptosis in the tumor tissues was independently verified by immunohistochemical staining for caspase 3, a downstream indicator of apoptosome-activated caspase-mediated apoptosis that would not cross-react with the caspase-9 PA probe. Figure 4(a) represents a control section stained with the sec-

ondary antibody alone (autofluorescence of the tissue without apparent staining); while, Fig. 4(b) shows the immunostaining of the caspase-3 p11 subunit (green) and the DAPI staining of cell nuclei. The intense green fluorescence in these sections suggests the wide spread apoptosis of cells in the tumor tissues after intravenous administration of high-dose cisplatin. In addition, cells on the peripheral of the tumor stained more strongly for caspase 3 (green fluorescence) compared to cells at the tumor interior. This was consistent with the PA imaging of apoptosis that showed strong apoptosis at the tumor peripheral, suggesting chemotherapeutics had penetrated the outer layers of the tumor and induced apoptosis.

In conclusion, we developed a cell-permeable imaging probe that can be utilized to monitor cancer cell apoptosis in living mice by photoacoustic imaging with improved contrast.

### Acknowledgments

We thank the National Institutes of Health (Grant Nos. P20RR016475, R21CA132033, R03DA026987, and 1R21EB010184) and the American Cancer Society (Grant No. RSG-0813301CDD) for support of these studies. In addition, S.C. was supported by a predoctoral fellowship from Eli Lilly. Thanks are extended to Jeff Krise (University of Kansas) for use of his microscopy facilities.

### References

1. K. H. Song and L. V. Wang, "Deep reflection-mode photoacoustic imaging of biological tissue," *J. Biomed. Opt.* **12**(6), 060503 (2007).
2. H. Cui, J. Staley, and X. Yang, "Integration of photoacoustic imaging and high-intensity focused ultrasound," *J. Biomed. Opt.* **15**(2), 021312 (2010).
3. J. Staley, P. Grogan, A. K. Samadi, H. Cui, M. S. Cohen, and X. Yang, "Growth of melanoma brain tumors monitored by photoacoustic microscopy," *J. Biomed. Opt.* **15**(4), 040510 (2010).
4. D. McCormack, M. Al-Shaer, B. S. Goldschmidt, P. S. Dale, C. Henry, C. Papageorgio, K. Bhattacharyya, and J. A. Viator, "Photoacoustic detection of melanoma micrometastasis in sentinel lymph nodes," *J. Biomech. Eng.* **131**(7), 074519 (2009).
5. R. Sadhukhan, J. W. Leone, J. Lull, Z. Wang, R. F. Kletzien, R. L. Heinrichson, and A. G. Tomasselli, "An efficient method to express and refold a truncated human procaspase-9: a caspase with activity toward Glu-X bonds," *Protein Expression Purif.* **46**(2), 299–308 (2006).
6. Y. Lu, Q. Yang, Y. Xie, S. Duan, S. Cai, and M. L. Forrest, "A sensitive near-infrared fluorescent probe for caspase-mediated apoptosis: synthesis and application in cell imaging," *Drug Discov. Ther.* (in press).
7. U. Haberkorn, R. Kinscherf, P. H. Krammer, W. Mier, and M. Eisenhut, "Investigation of a potential scintigraphic marker of apoptosis: radioiodinated Z-Val-Ala-DL-Asp(O-methyl)-fluoromethyl ketone," *Nucl. Med. Biol.* **28**(7), 793–798 (2001).